Nucleic Acids Research, 2025, **53**, gkaf1037
https://doi.org/10.1093/nar/gkaf1037
Nucleic Acid Therapeutics

MiR-ON-CRISPR: a microRNA-activated CRISPR–dCas9 system for precise gene therapy in living cells and mouse models of sepsis

Wen-Jie Shu[1,2,†], **Zhe Ma**[2,†], **Lijun Jia**[1,†], **Bin Guo**[2], **Xiaojie Tian**[2], **Chunxia He**[2], **Fu Wang**[1,2,*]

[1]Department of Medical Oncology, The Second Affiliated Hospital of Xi'an Jiaotong University, Xi'an, Shaanxi 710004, China
[2]Institute of Medical Engineering, Department of Biophysics, School of Basic Medical Sciences, Xi'an Jiaotong University, Xi'an 710061, China

*To whom correspondence should be addressed. Email: wangfu@xjtu.edu.cn
†The first three authors should be regarded as Joint First Authors.

Abstract

The CRISPR–dCas9 technology is a powerful tool for manipulating the expression of target genes in a variety of biomedical applications. Nevertheless, it is imperative that the activity of the CRISPR–dCas9 system be tightly controlled to improve its safety and applicability. In this study, we successfully designed a microRNA-activated CRISPR–dCas9 system, termed miR-ON-CRISPR, in which the core components (dCas9 and sgRNA) are both regulated by endogenous miRNA. Our findings demonstrated that the miR-ON-CRISPR system can regulate firefly luciferase reporter gene expression to faithfully visualize miRNA activity and image the differentiation status of neural cells. Moreover, the miR-ON-CRISPR was designed as an AND/OR gate system, thereby enabling the simultaneous detection of two distinct miRNAs. Furthermore, the system was adapted to achieve cell type-specific killing by activating the exogenous DTA genes or endogenous BAX genes. Finally, in mouse models of sepsis, the miR-ON-CRISPR system was shown to alleviate the sepsis-induced liver injury as well as the associated oxidative stress damage and endoplasmic reticulum stress via activating the nuclear erythroid 2-related factor 2 gene. In conclusion, this proof-of-concept study demonstrates the feasibility of the miR-ON-CRISPR system for cell type-specific control of CRISPR–dCas9 activity and its therapeutic applications in the treatment of genetic diseases.

Graphical abstract

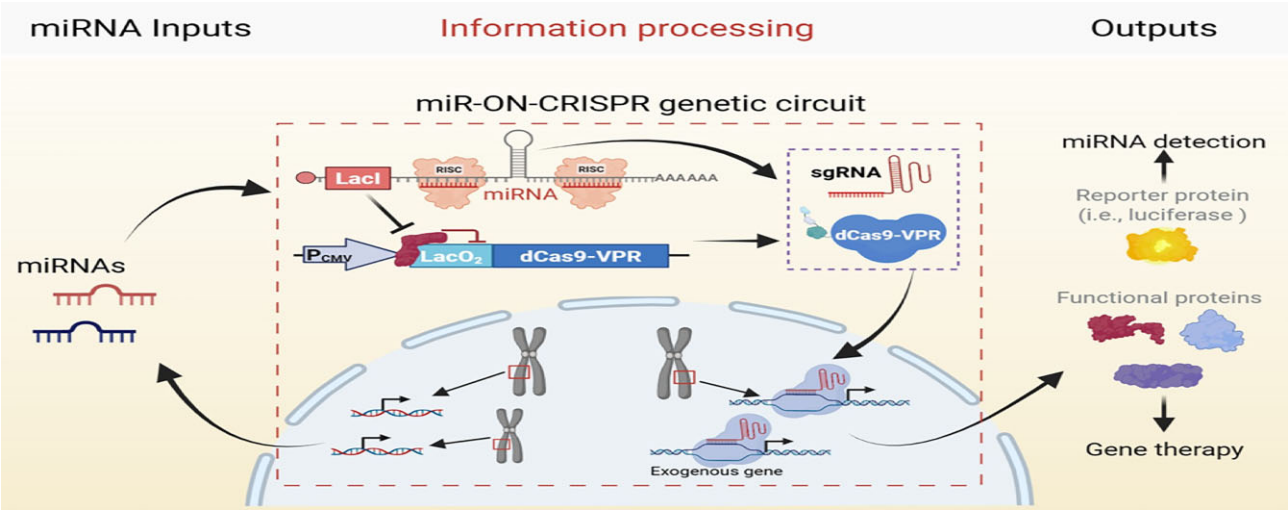

Introduction

The clustered regularly interspaced short palindromic repeats (CRISPR)/associated protein 9 (CRISPR/Cas9) gene editing technology represents a groundbreaking advancement in genetic engineering, offering immense potential for scientific research and therapeutic applications. This encompasses high-throughput screening, functional genomics research, and the investigation of conditions such as viral infections, genetic

Received: June 25, 2025. **Revised:** September 18, 2025. **Accepted:** September 19, 2025

diseases, and cancer. The nuclease-deficient Cas9 (dCas9) retains the ability to target genomic DNA without cleaving target DNA, making it a versatile tool for genome engineering. It is capable of forming various functional domains for tasks such as transcriptional regulation, gene imaging, and epigenetic modifications [1–4]. Nevertheless, like other CRISPR systems, the CRISPR–Cas9/dCas9 system exhibits recognized limitations, such as unanticipated off-target activity.

To improve the safety and applicability of CRISPR systems, the development of controllable CRISPR systems has been undertaken. These systems have been engineered to reduce off-target effects and genotoxicity by reducing the exposure time of the genome to the active system [5, 6]. Currently, two main strategies for controlling the activity of CRISPR systems have been shown to be efficacious: the design of Cas protein or guide RNA (gRNA) to be switchable. However, as is the case with most synthetic induction systems, single regulation of Cas protein or gRNA still exhibited some leaky activation of the system. Moreover, most of the switchable CRISPR systems demonstrate responsiveness to external signals, including light [7, 8] or small molecules [9], exhibiting a lack of cell specificity. In order to achieve the maximum potential of CRISPR systems, it is imperative to introduce genetic modules that can achieve tight and cell type-specific activation of the system.

MicroRNAs (miRNAs) are a class of endogenous noncoding RNAs that play important regulatory roles in a variety of biological processes [10]. A considerable number of miRNAs are expressed in a cell type-specific manner, and some of these have been identified as biomarkers of human cancers [11]. Besides, our previous studies have shown that the cell type-specific regulation of gene expression can be achieved by constructing miRNA-inducible systems [12–15]. This property paves the way for the development of a conditional CRISPR system that is activated exclusively in a specific cell type or disease state in response to endogenous miRNA signatures. In recent years, several miRNA-activated CRISPR systems have been reported by different research groups, including ours [15–20]. These studies demonstrated the feasibility of using miRNA as a cell type-specific endogenous signal to regulate CRISPR system activity.

The miRNA-inducible system has been proven to be applicable in various scenarios such as miRNA detection [13, 21], cell classification [22, 23], and cell type-specific regulation of CRISPR activity [15, 19]. Therefore, it is regarded as a good tool for cell type-specific regulation and has shown potential for application in both basic research and disease treatment. Among the existing systems, the miRNA-activated CRISPR systems were constructed by regulating the production of Cas9/dCas9 protein [15–17, 24, 25] or single guide RNA (sgRNA) [18–20, 26]. However, owing to the intrinsic characteristics of synthetic regulatory systems, these individual regulatory systems still exhibited leakage activity. That is to say, in the absence of target miRNA, the system maintained a certain degree of activity. Furthermore, most of these systems can only respond to one miRNA, which limits their ability to perform cell type-specific regulation.

In this study, we successfully constructed a smart system, designated as miR-ON-CRISPR, by integrating specific components into the 3′ untranslated region (UTR) of the LacI gene (Scheme 1). This integration entailed the insertion of miRNA target sites and short guide RNA (sgRNA) sequences, along with the incorporation of lac operator ($LacO_2$) sequences at the 5′ end of the dCas9-VPR gene. In contrast to earlier switchable CRISPR systems, the miR-ON-CRISPR system features a regulatory mechanism that is distinct from previous approaches. This regulatory mechanism involves the production of core components (dCas9 and sgRNA) by target miRNA. In the absence of target miRNA, functional sgRNA cannot be produced, and LacI inhibits dCas9-VPR expression via binding to the $LacO_2$, thus minimizing the leakage activity of the CRISPR system. In the presence of target miRNA, miRNAs would bind to the miRNA target sites, leading to the release of functional sgRNA through miRNA-mediated cleavage. The miRNA-mediated LacI mRNA degradation enables the expression of dCas9-VPR, which then activates the expression of the gene of interest (GOI) under the guidance of sgRNA. It is noteworthy that the miR-ON-CRISPR system exhibits minimal leakage activity in comparison to the single regulatory system, where only dCas9 or sgRNA can be switched. The miR-ON-CRISPR system has been demonstrated to accurately measure the activity of miRNAs and to image the differentiation status of neural cells. In addition, the system can be adapted to detect two miRNAs by designing an AND/OR gate system. Specifically, the system was adapted to achieve cell type-specific killing by designing sgRNAs that target the promoter regions of exogenous or endogenous apoptosis-related genes. Furthermore, in a mouse model of sepsis, the sepsis-induced liver injury could be alleviated by utilizing the system to trigger the expression of nuclear erythroid 2-related factor 2 (Nrf2) in the liver of mice. These findings underscore the efficacy of the proposed miR-ON-CRISPR system in the realm of potential gene-based therapeutic interventions.

Materials and methods

Plasmid construction

The required DNA fragments (Supplementary Table S1) were synthesized by Tsingke Biotechnology Co., Ltd. and subsequently cloned into the pCl-neo vector. Plasmid DNA was isolated from *Escherichia coli* using the EndoFree Mini Plasmid Kit II [TIANGEN BIOTECH (BEIJING) Co., Ltd., Beijing, China]. Sequencing was performed on all final plasmids to ensure sequence fidelity (Tsingke Biotechnology Co., Ltd.).

Cell cultures and transfection

Human cell lines HEK-293, HeLa, and P19 were cultured in dulbecco's modified eagle medium (DMEM) (Thermo Fisher Scientific) supplemented with 10% fetal bovine serum (FBS) (v/v), 100 U/ml penicillin, and 100 mg/ml streptomycin (Invitrogen). HCT-116 cells were cultured in RPMI1640 (Thermo Fisher Scientific) supplemented with 10% FBS (v/v), 100 U/ml penicillin, and 100 mg/ml streptomycin (Invitrogen). Cells were maintained at 37°C with 5% CO_2.

Plasmid transfections were performed using Lipo8000™ Transfection Reagent (Beyotime, Cat#C0533). Briefly, cells were trypsinized and seeded at a density of 1×10^5 cells per well in a 24-well plate with 0.5 ml of medium one day before transfection. Transfections were carried out at 70%–80% confluence. For each transfection, mix plasmid DNA gently by pipetting with 25 μl of Opti-MEM medium in a sterile tube, followed by adding Lipo8000™ Transfection Reagent. After gently mixing, the mixture is added to the cells.

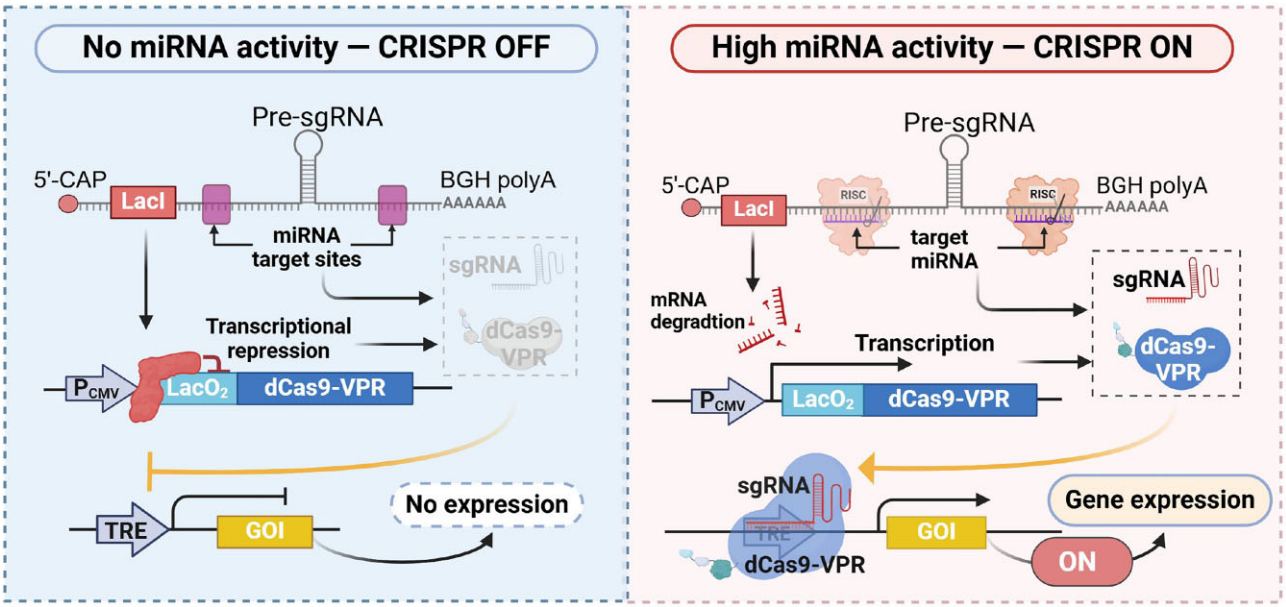

Scheme 1. A tight miRNA-inducible CRISPR–dCas9 system in which the production of dCas9 and sgRNA is regulated simultaneously. The system contains three components: a plasmid expressing LacI and pre-sgRNA (miRT-sgRNA-miRT), a plasmid expressing $LacO_2$-dCas9-VPR, and a TRE-GOI plasmid with the gene of interest (GOI) driven by a tetracycline response element (TRE). In the cells lacking target miRNA, functional sgRNA cannot be produced, and LacI protein expression inhibits dCas9-VPR expression via binding to the $LacO_2$ site, thus minimizing the leakage activity of the CRISPR system. In the presence of target miRNAs, functional sgRNA can be released through miRNA-mediated cleavage, and the miRNA-mediated LacI mRNA degradation enables the expression of dCas9-VPR. Then, the dCas9-VPR could activate the expression of GOI under the guidance of sgRNA targeting TRE.

For plasmid DNA and miRNA mimic co-transfection, Lipofectamine 2000 (Thermo Fisher Scientific) transfection reagent was used. Plasmid DNA and miRNA mimics were diluted in Opti-MEM and mixed with diluted Lipofectamine 2000. After incubation, the mixture was added to each well, and the culture medium was replaced after 6 h. The miRNA mimics used in this study were obtained from GenePharma (Supplementary Table S2).

sgRNA design

To design effective sgRNA and minimize off-targets, an online CRISPR design tool was used (https://benchling.com). This online tool can design multiple sgRNAs based on the target sequence and calculate the on-target score and off-target score for each sgRNA according to the reported methods [27, 28]. After comprehensively considering the on-target score and the off-target score, a specific sgRNA was selected for the experiment. The full sgRNA sequences are listed in Supplementary Table S2.

P19 cell differentiation

Retinoic acid (RA) was prepared as a 5-μM stock solution using dimethyl sulfoxide (DMSO) and then diluted 1000-fold into prepared DMEM medium. P19 cells were cultured in 24-well plates and incubated for 24 h. Subsequently, the cell medium was replaced with RA-supplemented medium every 2 days. P19 cells were harvested at the 0-, 2-, 4-, and 6-day time points of differentiation.

Luciferase activity assay

After 36–48 h of transfection, cells were washed with phosphate buffered saline (PBS), and lysis buffer was added to lyse the cells. Following incubation and centrifugation, supernatants were collected. Luciferase activity was measured by adding lysate and firefly luciferase detection reagent (YEASEN, Cat:11401ES76) to a 96-well plate, followed by luminescence intensity measurement using a multimode reader.

RNA extraction and real-time quantitative PCR

Total RNA was isolated from cells or tissues using the SPARKeasy Improved Tissue/Cell RNA Kit (Sparkjade, Cat#AC0202), and complementary DNA (cDNA) was synthesized using the Reverse Transcription Kit (TianGen, Beijing) from 500 ng of total RNA. For miRNA detection, the SPARKScriptII miRNA 1st strand cDNA synthesis kit (by stem-loop) (Sparkjade, Cat#AG0502) was used to synthesize cDNA. Real-time quantitative PCR (RT-qPCR) was performed using SYBR Green qPCR Master Mix (Biosharp, Cat#BL698A). Relative gene expression was calculated using the $2^{-\Delta\Delta CT}$ method with GAPDH or U6 as the reference for normalization. Primer sequences are listed in Supplementary Table S3.

Flow cytometry analysis

Cell samples were prepared using an Annexin V-FITC/PI Apoptosis Detection Kit (YEASEN, Cat#40302ES50). Briefly, cells were digested with ethylenediaminetetraacetic acid-free 0.1% trypsin and collected in a centrifugal tube. After being washed twice with ice-cold PBS, the cells were centrifuged for 5 min at 500 × *g* at 4°C. The supernatant was discarded and the cell pellets were resuspended in binding buffer. The 100 μl cell suspension was added to Annexin V-FITC solution and 10 μl PI solution. After incubation for 15 min, the samples were analyzed by flow cytometry.

Sepsis mouse model

ICR mice (male, 5–6 weeks old) were purchased from the Laboratory Animal Center of Xi'an Jiaotong University. All animal experiments are conducted in accordance with the guidance of the Institutional Animal Care and Use Committee at Xi'an Jiaotong University. To establish lipopolysaccharide (LPS)-induced sepsis mouse model, LPS (Beyotime, Cat#S1732) was dissolved and diluted to 2 mg/ml (20 mg/kg) for intraperitoneal injection. Body weight and body temperature were monitored before and after LPS injection. The blood and liver tissues of sepsis mice were collected for downstream analysis.

Detection of cytokines and hepatic transaminases

The levels of circulating cytokines TNF-α and IL-6 in serum of mice were assessed by ELISA kits (Epizyme Biotech, China) following the manufacturer's instructions. Serum level of ALT and AST was determined by the Alanine aminotransferase Assay Kit and the Aspartate aminotransferase Assay Kit (Nanjing Jiancheng Bioengineering Institute, China) according to the manufacturer's instructions.

Detection of hepatic oxidative stress, endoplasmic reticulum stress, and hepatocyte apoptosis

The malondialdehyde (MDA) levels were measured according to the instructions of the MDA test kit (Servicebio, China). Terminal deoxynucleoitidyl transferase dUTP nick end labeling (TUNEL) staining was performed on the tissues to determine apoptosis. For statistical analysis of TUNEL, 10 fields were observed from one slide, and TUNEL-positive cells were counted for comparison. Immunohistochemical (IHC) staining was used to detect the expression levels of endoplasmic reticulum (ER) stress and apoptosis-related protein markers. Liver tissue of the mice was harvested and fixed with 4% paraformaldehyde fixative, then the tissue was provided to Servicebio Biotechnology Ltd. for testing in the usual procedure. Ten fields of each sample were observed for statistical analysis. The percentage of IHC staining positive cells was divided into four categories, and the staining intensity was divided into four grades: 0 (none), 1 (weak), 2 (moderate), and 3 (strong). The final stain score of IHC is defined as the product of the percentage and intensity score.

Statistical analysis

All experiments were independently performed in triplicate, and data are presented as mean ± SD. Statistical significance between experimental groups was determined using Student's *t*-tests. $^{*}P < .05$, $^{**}P < .01$, $^{***}P < .001$, and "ns" indicates "not significant."

Results and discussion

Design and characterization of miRNA-activated dCas9 or sgRNA system

We previously developed an LacI-based miRNA-inducible genetic circuit for miRNA detection and cell type-specific gene activation [12, 21]. Inspired by this, we suspected that the LacI repression system could also be used to activate dCas9 expression, thereby regulating the activity of the corresponding CRISPR system. Consequently, an miRNA-activated dCas9 system (miR-ON-dCas9) was constructed based on the LacI repression system. In the miR-ON-dCas9 system, the miRNA target sites (miRNA-TS) and two copies of the $LacO_2$ sequences were inserted into the 3′-UTR of the LacI gene or the front of dCas9-VPR gene, respectively. The firefly luciferase (Fluc) gene, driven by a tetracycline-inducible promoter, serves as a reporter gene (TRE-Fluc) for CRISPR activity (Fig. 1A). In the dCas9-VPR protein [29], three transcriptional activators (VP64, P65, and RTA) are fused to the C-terminal of dCas9, thereby effectively activating the target gene. As shown in Fig. 1A, the presence of target miRNAs was found to be a prerequisite for the degradation of the LacI repressor, thus enabling the expression of dCas9-VPR protein and, consequently, the formation of a transcriptional activation complex that would result in the activation of Fluc expression.

To test the feasibility and specificity of the system, a miR21-activated dCas9-VPR system (miR21-ON-dCas9) was constructed. The miR21-ON-dCas9 system plasmids were then co-transfected with miR-1, miR-9, miR-21, or miR-124 mimics into HEK293 cells, which did not express these endogenous miRNAs. As indicated by the Fluc activity, the system was only activated by target miR-21 mimics, but not non-targeted miRNA mimics (Fig. 1B). Furthermore, to evaluate whether the system could be activated by endogenous target miRNA, we tested the system in several cell lines that either expressed or did not express miR-21. Consistent with previous studies [19, 30], the luciferase assay showed that HEK293 cells had negligible miR-21 activity, while HeLa and HCT116 cells exhibited strong miR-21 activity (Supplementary Fig. S1A and B). Then, a control group lacking miR-21 target sites was designed (Supplementary Fig. S1C). Following the transfection of control or miR21-ON-dCas9 plasmids into various cell lines, distinct activation of Fluc expression was observed. Specifically, Fluc expression was significantly induced in HeLa and HCT-116 cells exhibiting high levels of endogenous miR-21, but not in HEK-293 cells, which did not express endogenous miR-21 (Fig. 1C–E). Furthermore, an elevated Fluc expression was observed in HeLa cells in response to the increased transfection of miR21-ON-dCas9 plasmids (Supplementary Fig. S1D). These data suggest that the miR-ON-dCas9 system can be activated by endogenous target miRNAs.

In addition, we also designed an miRNA-activated sgRNA system (miR-ON-sgRNA), in which the production of functional sgRNAs is regulated by a target miRNA. In the absence of target miRNAs, the pre-sgRNAs are designed to be transcribed by RNA polymerase II. Consequently, the 5′ cap and 3′ polyA-tail structures in the transcripts will prevent them from being processed into functional sgRNAs. Conversely, when target miRNAs are present, mature sgRNAs are released by RNA-induced silencing complex-mediated cleavage, which then activates the expression of the Fluc reporter gene via the formation of a transcriptional activation complex with dCas9-VPR (Fig. 1F). Subsequently, a miR21-activated sgRNA system (miR21-ON-sgRNA) was constructed by inserting corresponding miR-21 target sites at both ends of the sgRNA. The miR21-ON-sgRNA system plasmid was co-transfected into HEK-293 cells with several miRNA mimics, respectively, and the results showed that Fluc could only be activated by the target miR-21 mimics (Fig. 1G). Moreover, the miR21-ON-sgRNA system was activated in HeLa or HCT116 cells that expressed high levels of miR-21, but not in HEK293 cells that did not express endogenous miR-21 (Fig. 1H–J). The luciferase signal of the miR21-ON-sgRNA

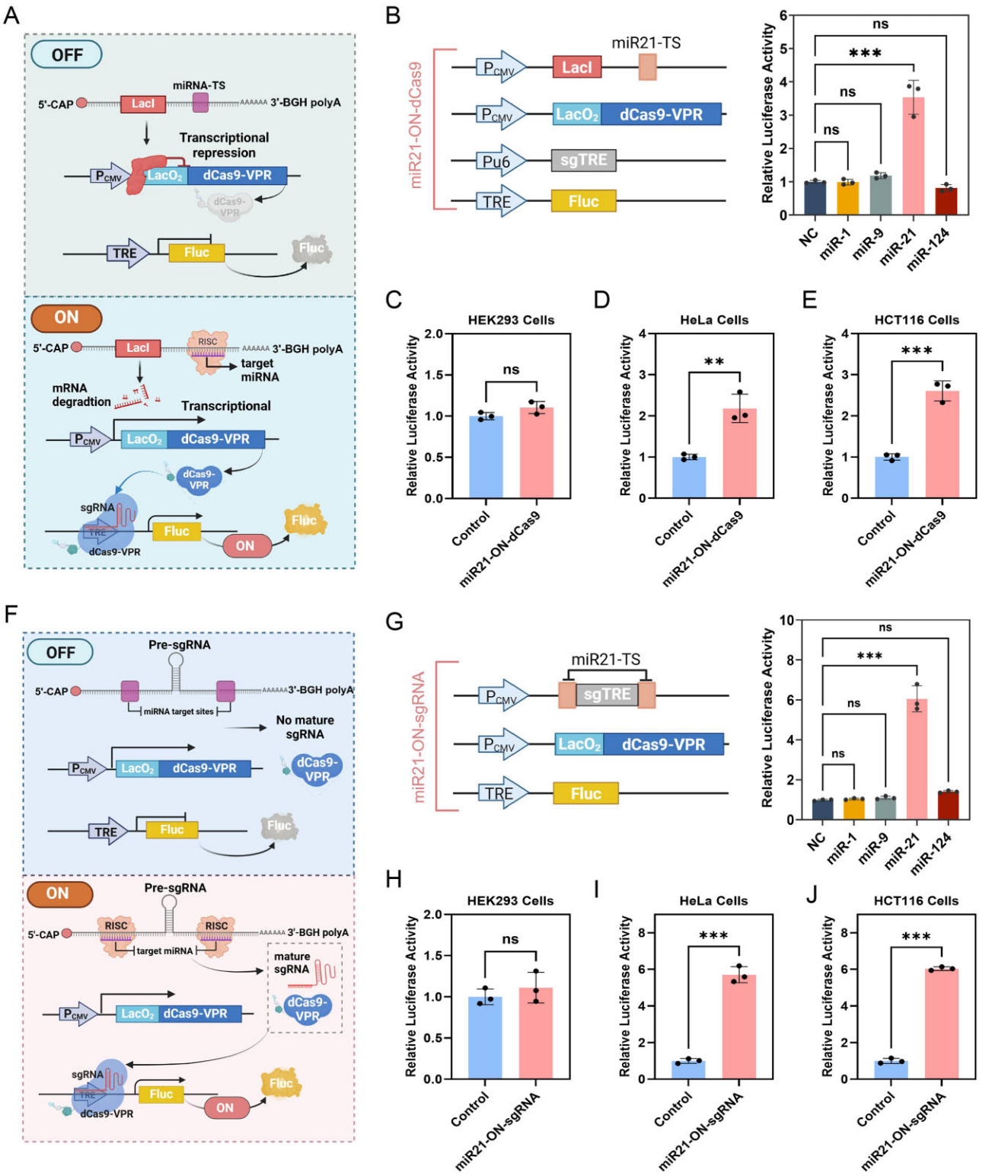

Figure 1. Design and characterization of the miRNA-activated dCas9-VPR or sgRNA system. (**A**) Scheme for the miR-ON-dCas9 system that contains three components: a plasmid expressing the LacI in which the miRNA target site is inserted into the 3′-UTR of the LacI, a plasmid expressing LacO2-dCas9-VPR, and a TRE-Fluc plasmid with the Fluc gene driven by a tetracycline-inducible promoter. (**B**) miR21-ON-dCas9 system plasmids were co-transfected with indicated miRNA mimics, respectively, and the luciferase activity was measured. (**C**–**E**) The control or miR21-ON-dCas9 system plasmids were transfected into the indicated cells, and the luciferase activity was measured. (**F**) Scheme for the miR-ON-sgRNA system that contains three components: a plasmid expressing pre-sgRNA (miRT-sgRNA-miRT), a plasmid expressing dCas9-VPR, and a TRE-Fluc plasmid with the Fluc gene driven by a tetracycline-inducible promoter. (**G**) miR21-ON-sgRNA system plasmids were co-transfected with indicated miRNA mimics, respectively, and the luciferase activity was measured. (**H**–**J**) The control or miR21-ON-sgRNA system plasmids were transfected into the indicated cells, and the luciferase activity was measured.

system also exhibited a dose-dependent increase in HEK293 cells (Supplementary Fig. S1E and F). These results suggest that cell type-specific miRNAs can function as an endogenous signal to activate CRISPR systems by modulating the production of sgRNA.

Design and characterization of miRNA-activated CRISPR–dCas9 dual regulatory system

In order to obtain a tight miRNA-activated CRISPR–dCas9 system with minimal leakage expression, a further design of a dual regulatory system (miR-ON-CRISPR) was made based on the miR-ON-dCas9 and miR-ON-sgRNA systems. Within this dual regulatory system, the production of dCas9-VPR and sgRNA is subject to regulation by endogenous target miRNAs, thereby minimizing leakage expression and genotoxicity of the CRISPR system. In the presence of target miRNAs, miRNA-mediated cleavage promotes the expression of dCas9-VPR and releases functional sgRNAs, which in turn activate the CRISPR system, as evidenced by the measurement of Fluc activity (Fig. 2A). To test the feasibility of the miR-ON-CRISPR system, a miR21-activated dCas9-VPR and sgRNA system (miR21-ON-CRISPR) was constructed (Fig. 2B). As indicated by the Fluc activity, the system can be activated by target miR-21 mimics, but no other nontargeted miRNA mimics (Fig. 2C and Supplementary Fig. S2A). Furthermore, an increase in the degree of activation of the system was observed with an increase in the dosage of target miRNA (Fig. 2D).

Next, to test the off-target activity of the miR21-ON-CRISPR system, we constructed an intentionally off-target TRE-Fluc by mutating three bases. The results showed that in this case, the system could not be activated by the target miR-21 (Fig. 2E). In addition, the system can only be activated by the target miR-21 when it has the miR-21 recognition sites (Fig. 2F and Supplementary Fig. S2B). These results indicate that the miR-ON-CRISPR system exhibits excellent miRNA response specificity and low off-target activity.

In order to ascertain the universality of the miR-ON-CRISPR system, a miR124-activated CRISPR system (miR124-ON-CRISPR) was constructed on the basis of the miR-ON-CRISPR system. In a manner analogous to the miR21-ON-CRISPR system, the miR124-ON-CRISPR system was shown to be specifically activated by target miR-124 mimics (Fig. 2G and H). In addition, the miR-ON-CRISPR system was demonstrated to be effective in a C2C12 myoblast cell line that is relatively difficult to transfect (Supplementary Fig. S2C–F). Furthermore, the activity of the miR21-ON-CRISPR system was examined in various cell lines (HeLa and HCT116 cells). It was found that the system can be effectively activated by endogenous target miRNA-21 in a dose-dependent manner (Supplementary Fig. S3A–D). Notably, the leakage activity of the miR21-ON-CRISPR system was found to be negligible in comparison to that of the two single regulatory systems, miR21-ON-dCas9 and miR21-ON-sgRNA (Fig. 2I). Similar to the miRNA dose-activation effect shown by the miR-ON-CRISPR system (Fig. 2D and H), the activation of the miR-ON-sgRNA and miR-ON-dCas9 systems may also have an miRNA dose-dependent effect. However, it is believed that this dual-regulated miR-ON-CRISPR system would have a lower background signal because it shows extremely low leakage expression (Fig. 2I). Collectively, these data suggest that the miR-ON-CRISPR system is an effective cell type-specific CRISPR–dCas9 regulatory tool with negligible leaky activity.

Monitor the activity of miR-124 during neural cell differentiation with the miR-ON-CRISPR system

To further explore the applicability of the miR-ON-CRISPR system, we tested whether the system could be used to monitor the activity of endogenous miRNA. To this end, the P19 neural cell differentiation model was used to verify the capacity of the miR-ON-CRISPR system to visualize the activity of miR-124 (Fig. 3A), the expression of which is reported to increase during neural cell differentiation [31]. Subsequently, the miR124-ON-CRISPR system plasmids were transfected into differentiating P19 cells. The results showed that the expression of Fluc increased gradually with the progression of differentiation time (Fig. 3B and C). Furthermore, the expression of miR-124 during the cellular differentiation was detected by qPCR assay. Consistently, the result showed the expression of miR-124 was gradually increased during the process of cell differentiation (Fig. 3D). Next, we tested whether the system can be used to monitor the differentiation status by means of imaging the expression level of miR-124. As expected, an elevated bioluminescence signal was observed during the process of cell differentiation (Fig. 3E and F). These findings demonstrated the effectiveness of the miR-ON-CRISPR system in real-time imaging of miRNAs and its associated biological processes, such as cell differentiation.

"OR/AND-gated" miR-ON-CRISPR system enables detecting the expression of two miRNAs

Despite the fact that the expression of many miRNAs is cell type-specific, there are some cases in which the integration of multiple miRNAs' signals is necessary to achieve optimal cell type-specific regulation of the CRISPR system. Consequently, the subsequent investigation focused on determining whether the miR-ON-CRISPR system could be adapted to detect two distinct miRNAs. It has been demonstrated by our and others' studies that the insertion of miRNA target sites into either the 5′-UTR or 3′-UTR of target genes is an effective procedure [12, 21, 32]. To ascertain the potential of this feature for the regulation of CRISPR activity, two additional miRNA-activated systems were constructed, in which the target sites of miR-21 were inserted into either the 5′-UTR (T21-LacI) (Supplementary Fig. S4A) or both the 5′-UTR and 3′-UTR (T21-LacI-T21) of the LacI gene (Supplementary Fig. S4B). The results showed that the two types of systems can be activated by either exogenous or endogenous target miR-21 (Supplementary Fig. S4A and B). In addition, the system containing miR-21 target sites within both the 5′-UTR and 3′-UTR exhibited the highest fold-change in luciferase activity compared to the systems containing miR-21 target sites within the 5′-UTR or 3′-UTR following the introduction of miR-21 into HEK293 cells (Supplementary Fig. S4C). These results suggested that an miRNA-activated dCas9 system can be achieved by inserting miRNA target sites into either the 5′-UTR or 3′-UTR of the LacI gene.

Subsequently, an "OR-gated" miR-ON-CRISPR system (miR-OR-ON-CRISPR) was designed, in which miR21- and miR124-activated sgRNA modules were inserted into the 5′-UTR and 3′-UTR of the LacI gene, respectively (Fig. 4A). Subsequently, the system plasmids were co-transfected into HEK293 cells with either miR-21 or miR-124 mimics, or both

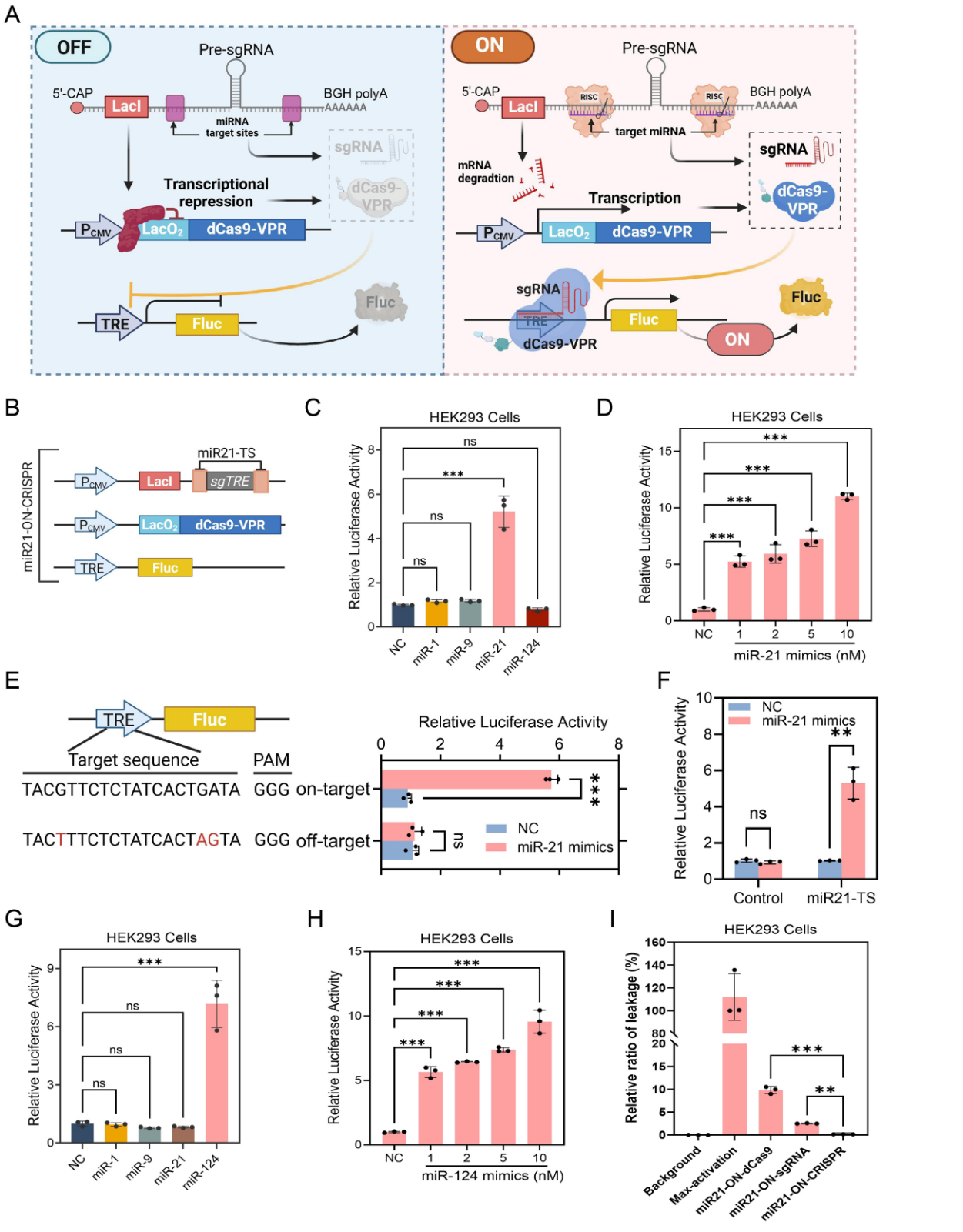

Figure 2. Design and characterization of the miR-ON-CRISPR system. (**A**) Scheme for the miR-ON-CRISPR system. (**B**) Three components of the miR21-ON-CRISPR system. (**C**) miR21-ON-CRISPR system plasmids were co-transfected with indicated miRNA mimics, respectively, and the luciferase activity was measured. (**D**) The miR21-ON-CRISPR system plasmids and different doses of miR-21 mimics were co-transfected into HEK293 cells. Then, the luciferase activity was measured 36 h later. (**E**) The off-target activity of the miR21-ON-CRISPR system was detected. (**F**) The activation of the system was detected in the presence or absence of miR-21 recognition sites. (**G**) miR124-ON-CRISPR system plasmids were co-transfected with indicated miRNA mimics, respectively, and the luciferase activity was measured. (**H**) The miR124-ON-CRISPR system plasmids and different doses of miR-124 mimics were co-transfected into HEK293 cells. Then, the luciferase activity was measured 36 h later. (**I**) The miR21-ON-dCas9, miR21-ON-sgRNA, and miR21-ON-CRISPR system plasmids were transfected in HEK293 cells to detect the leakage activity. Max-activation indicates transfection of a CRISPR system that consistently expresses sgRNA and dCas9-VPR. The expression of Fluc in the Max-activation state is defined as 100% leaky expression.

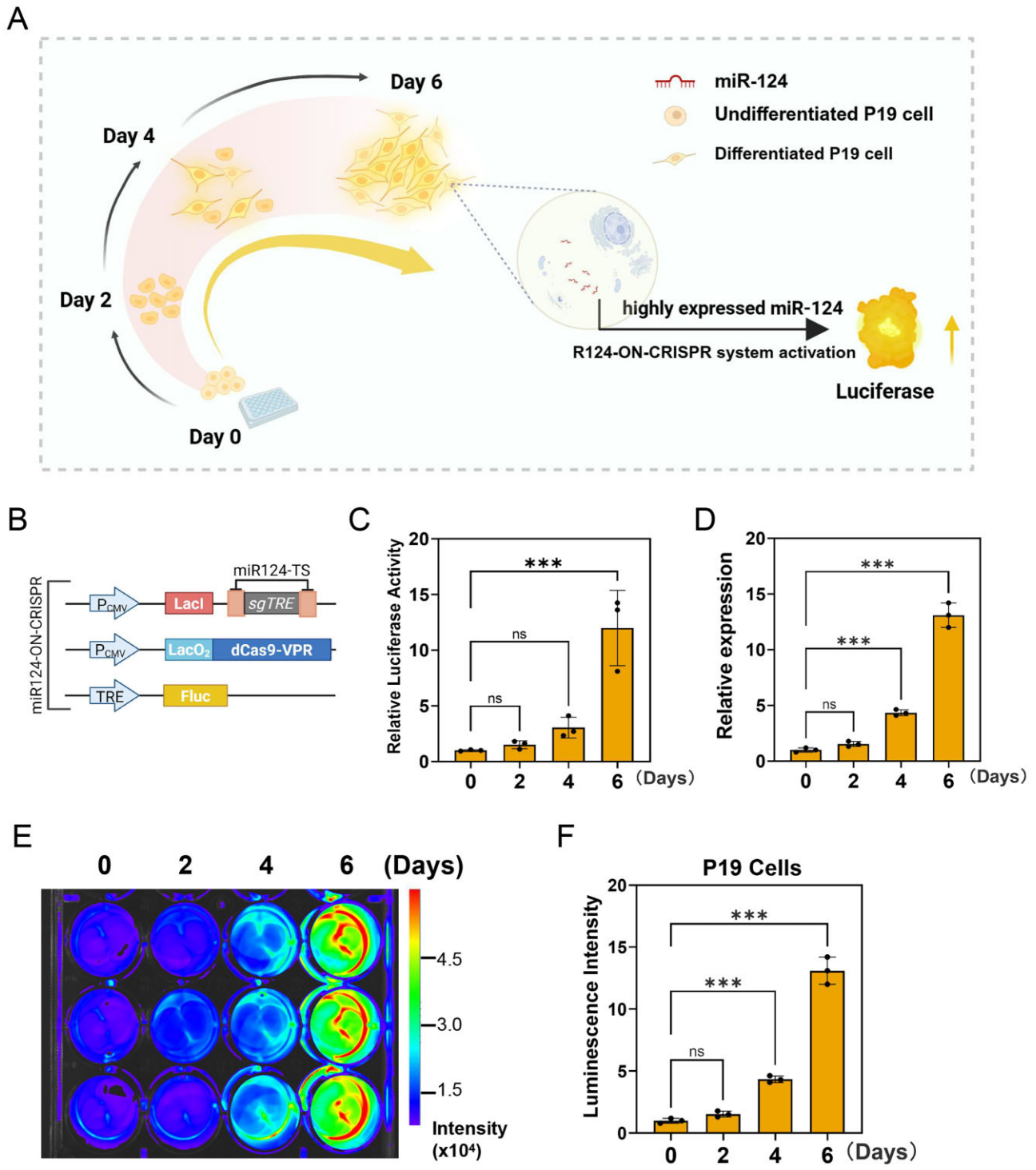

Figure 3. miR-ON-CRISPR system is used to visualize miRNA expression during cell differentiation. (**A**) Scheme for real-time detection of miRNA-124 in neurogenesis using the miR124-ON-CRISPR system. (**B**) Three components of the miR124-ON-CRISPR system. (**C**) The miR124-ON-CRISPR system plasmids were transfected into differentiated P19 cells at various time periods, and the luciferase activities were measured. (**D**) qPCR was performed to measure the expression level of miRNA-124 in differentiated P19 cells on different days. The miR124-ON-CRISPR system plasmids were transfected into differentiated P19 cells at various time periods; the bioluminescence signal (E) and luminescence intensity (F) were captured.

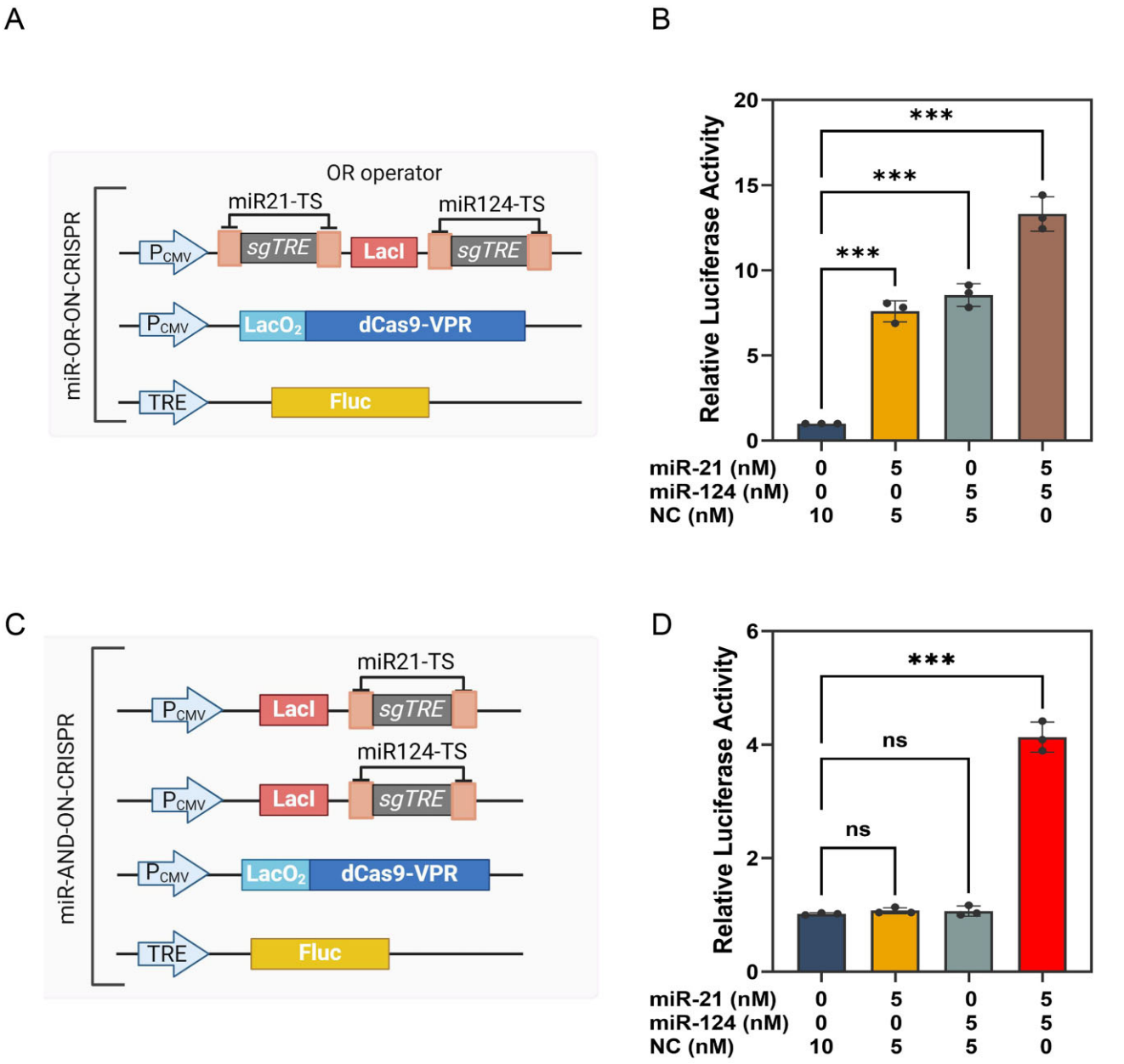

Figure 4. "OR/AND-gated" miR-ON-CRISPR system enables detecting the expression of two miRNAs. (**A**) Schematic diagram of the components of the miR-OR-ON-CRISPR system, which can be activated by either miR-21 or miR-124. (**B**) miR-OR-ON-CRISPR system plasmids were co-transfected with indicated miRNA mimics, respectively, and the luciferase activity was measured. (**C**) Schematic diagram of the components of the miR-AND-ON-CRISPR system, which is activated only in the presence of miR-21 and miR-124. (**D**) miR-AND-ON-CRISPR system plasmids were co-transfected with indicated miRNA mimics, respectively, and the luciferase activity was measured.

miR-21 and miR-124 mimics. As anticipated, transfection of either miR-21 or miR-124 mimics was found to activate the system, with the highest activation being observed when simultaneous transfection of miR-21 and miR-124 mimics (Fig. 4B). Furthermore, by inserting miR21- and miR124-activated sgRNA modules into the 3′-UTR of the LacI gene separately, an "AND-gated" miR-ON-CRISPR system (miR-AND-ON-CRISPR) was successfully constructed (Fig. 4C). As indicated by luciferase activity, the miR-AND-ON-CRISPR system can be activated only when transfecting miR-21 and miR-124 mimics simultaneously (Fig. 4D). Together, these results indicate that the miR-ON-CRISPR system can be engineered to detect the expression of two miRNAs.

miR-ON-CRISPR system induces cell type-specific apoptosis by activating the exogenous or endogenous toxic genes

Next, we explored whether the system could be activated by cell type-specific miRNA to regulate the expression of genes with biological functions. Given that toxic genes typically require low levels of leakage expression [33], it is suspected that the miR-ON-CRISPR system is well suited to regulate the expression of such genes. Therefore, the miR-ON-CRISPR system was designed to modulate the expression of the diphtheria toxin A (DTA) gene, which has been demonstrated to inhibit protein synthesis and induce apoptosis (Fig. 5A). Subsequently, an miR21-activated DTA expression

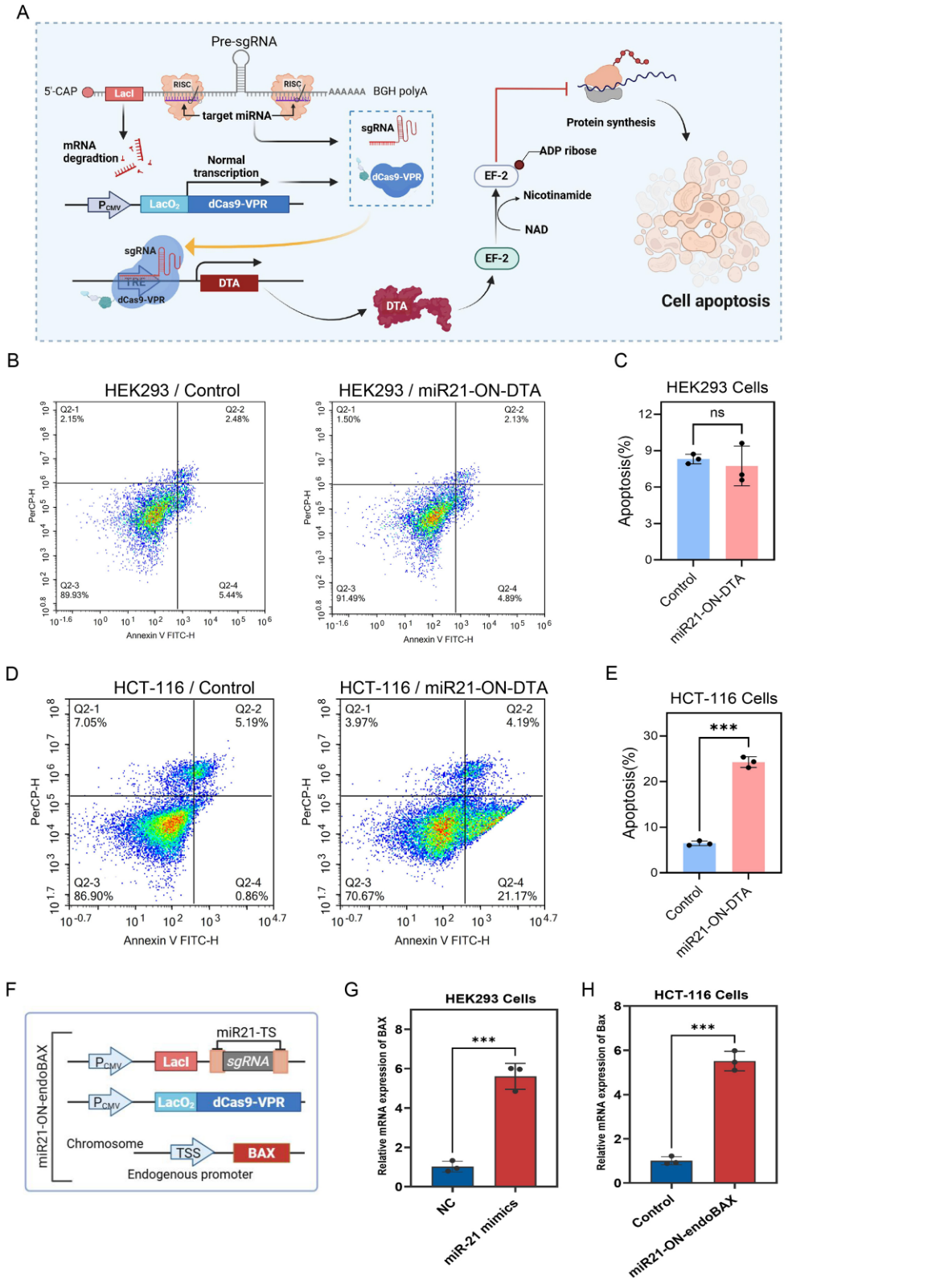

Figure 5. miR-ON-CRISPR system activates the expression of exogenous or endogenous toxic genes induced by cell type-specific miRNA. (**A**) Schematic diagram of the expression of toxic gene DTA induced by the miR-ON-CRISPR system to trigger cell apoptosis. (**B**–**E**) Flow cytometric analyses and quantification of cell apoptosis in (B and C) HEK293 or (D and E) HCT116 cells transfected with control or miR21-ON-DTA plasmids. (**F**) Schematic diagram of the components of the miR21-ON-endoBAX system, which can be used to activate the expression of endogenous BAX gene. (**G** and **H**) miR21-ON-endoBAX system plasmids were co-transfected with miR-21 mimics into HEK293 cells or alone transfected into HCT116 cells, and the mRNA expression of Bax was measured by qPCR.

system (miR21-ON-DTA) was constructed based on the miR-ON-CRISPR system. To verify the effectiveness of the miR21-ON-DTA system, flow cytometry analysis was performed to detect cell apoptosis under different transfection conditions. As indicated in Fig. 5B and C, in HEK293 cells (no endogenous miR-21 cells), the expression of the miR21-ON-DTA system plasmids did not induce more apoptosis compared with the control group (Supplementary Fig. S5A). In HCT-116 (Fig. 5D and E) or HeLa cells (Supplementary Fig. S5B and C) that express high levels of endogenous miR-21, the transfection of the miR21-ON-DTA plasmids resulted in a significant increase in apoptosis. These results demonstrate that the miR-ON-CRISPR system can induce cell type-specific apoptotic death by activating the expression of exogenous toxic genes.

Furthermore, by redesigning a conditional sgRNA targeting the endogenous promoter of BAX gene, a miR21-activated BAX expression system (miR21-ON-endoBAX) was constructed based on miR-ON-CRISPR system (Fig. 5F). In the miR21-ON-endoBAX system, target miRNA can activate the expression of endogenous BAX gene, then the expressed Bax protein will disrupt mitochondrial transmembrane potential and lead to the release of cytochrome c, thereby mediating caspase activation and ultimately inducing cell apoptosis (Supplementary Fig. S6A). As expected, following transfecting the system plasmids into HEK293 cells, the expression of the on-target BAX gene could be activated by exogenous miR-21 mimics (Fig. 5G), while the most likely off-target genes were not activated (Supplementary Fig. S6B). Moreover, the mRNA expression of BAX can also be activated by endogenous miR-21 in HCT-116 cells (Fig. 5H). Consistently, the presence of exogenous miR-21 mimics in HEK293 cells (Supplementary Fig. S6C and D) or endogenous miR-21 in HCT-116 cells (Supplementary Fig. S6E and F) has been shown to result in a significant increase in cell apoptosis. Together, these data suggest that the miR-ON-CRISPR system can be adapted to achieve cell type-specific killing by modulating the expression of either exogenous or endogenous toxic genes.

miR-ON-CRISPR system alleviates sepsis-induced symptoms in mice

Given the growing body of evidence indicating that numerous miRNAs are effective biomarkers for human diseases, it is hypothesized that the miR-ON-CRISPR system may offer significant therapeutic potential in the treatment of specific diseases through gene therapy. Sepsis is a life-threatening disease caused by dysregulation of the body's response, which poses a significant challenge in clinical treatment. Sepsis is characterized by multiple organ dysfunction, of which liver injury is a common occurrence [34]. In the clinic setting, sepsis-induced liver injury is closely related to mortality and poor prognosis in patients with sepsis [35]. In addition, the transcription factor Nrf2 exerts a protective effect on sepsis-induced liver injury by promoting the expression of antioxidant enzymes [36, 37]. Furthermore, miRNAs have been identified as biomarkers for sepsis [38]. As one of the miRNA biomarkers, the expression of miR-155 was shown to be significantly elevated in the liver during sepsis [39, 40]. Therefore, it is hypothesized that the design of miR-155 capable of activating the expression of the Nrf2 gene during sepsis may alleviate the sepsis-induced liver injury.

To test this hypothesis, we first established a mouse sepsis model by intraperitoneal injection of LPS (Fig. 6A). Consistent with previous studies, the injection of LPS for a duration of 6 or 12 h effectively induced a sepsis phenotype in mice, characterized by a decrease in body weight (Fig. 6B) and an increase in the levels of circulating cytokines such as TNF-α (Fig. 6C) and IL-6 (Fig. 6D). In addition, following treatment with LPS, the livers of the mice became darker and some bleeding spots appeared, indicating that sepsis had affected the liver (Fig. 6E). Elevated serum ALT and AST levels (Fig. 6F) and the HE staining of liver tissue (Fig. 6G) further indicated that sepsis caused liver injury. These results suggest that the mouse model of sepsis has been established successfully.

Then, we constructed a miR155-activated Nrf2 expression system (miR155-ON-Nrf2) based on the miR-ON-CRISPR system (Fig. 7A). To assess the performance of the miR155-ON-Nrf2 system in sepsis, the system plasmids were delivered to the mice's liver by hydrodynamic injection via the tail vein, and the mice were further intraperitoneally injected with LPS to induce sepsis (Fig. 7B). Consistent with previous studies [39, 40], the expression of miR-155 increased after LPS treatment (Supplementary Fig. S7A). Moreover, LPS-induced sepsis resulted in the activation of Nrf2 mRNA expression in the livers of mice (Fig. 7C). This finding suggests that miR-155 successfully activates the miR155-ON-Nrf2 system. Notably, the expression of the miR155-ON-Nrf2 system was capable of reversing the decreased body weight and body temperature caused by LPS injection (Supplementary Fig. S7B and C). In addition, LPS treatment led to an increase in pro-inflammatory factors TNF-α and IL-6, indicating the successful establishment of the model (Fig. 7D and E). Besides, the concentrations of pro-inflammatory cytokines TNF-α and IL-6 in circulation were decreased in sepsis mice expressing the miR155-ON-Nrf2 system plasmids (Fig. 7D and E). These data suggest that the miR155-ON-Nrf2 system has the potential to alleviate the sepsis symptoms in mice.

To further verify that the reduction of symptoms in sepsis is indeed caused by the expression of the Nrf2, we examined the expression of several antioxidative enzyme genes, including NQO1, GCLM, and HO-1, which can be activated by Nrf2 [41, 42]. Perhaps as a transient stress response, the expressions of NQO1 and GCLM were decreased, while the expression of HO-1 was increased in septic mice, which was similar to the results of a previous study [36]. Importantly, the expressions of these three antioxidant enzyme genes were all upregulated in sepsis mice expressing the miR155-ON-Nrf2 system plasmids (Fig. 7F). In addition, by measuring MDA levels in liver tissue, it was found that LPS treatment resulted in increased hepatic oxidative stress, while Nrf2 expression reduced the oxidative stress levels (Fig. 7G). Consistent with this finding, IHC analysis showed an increased expression of superoxide dismutase SOD1 in sepsis mice expressing Nrf2 (Supplementary Fig. S7D and E).

Previous studies have shown that oxidative stress could induce ER stress to mediate apoptosis [43], so we further investigated the role of miR155-ON-Nrf2 system in ER stress and cell apoptosis in septic liver tissues. By analyzing the expression of ER stress markers CHOP, GRP78, and ATF-6 in livers, it was shown that the expression of Nrf2 can also reduce ER stress in sepsis (Supplementary Fig. S8A-C). Moreover, TUNEL staining showed that the expression of the miR155-ON-Nrf2 system reduced the apoptotic ratio of hepatocytes in sepsis mice (Supplementary Fig. S9A and B). Consistently, a decreased expression of Bax and cleaved caspase3 was observed in sepsis mice expressing system plasmids (Supplementary Fig. S9C-F). These results suggested that the

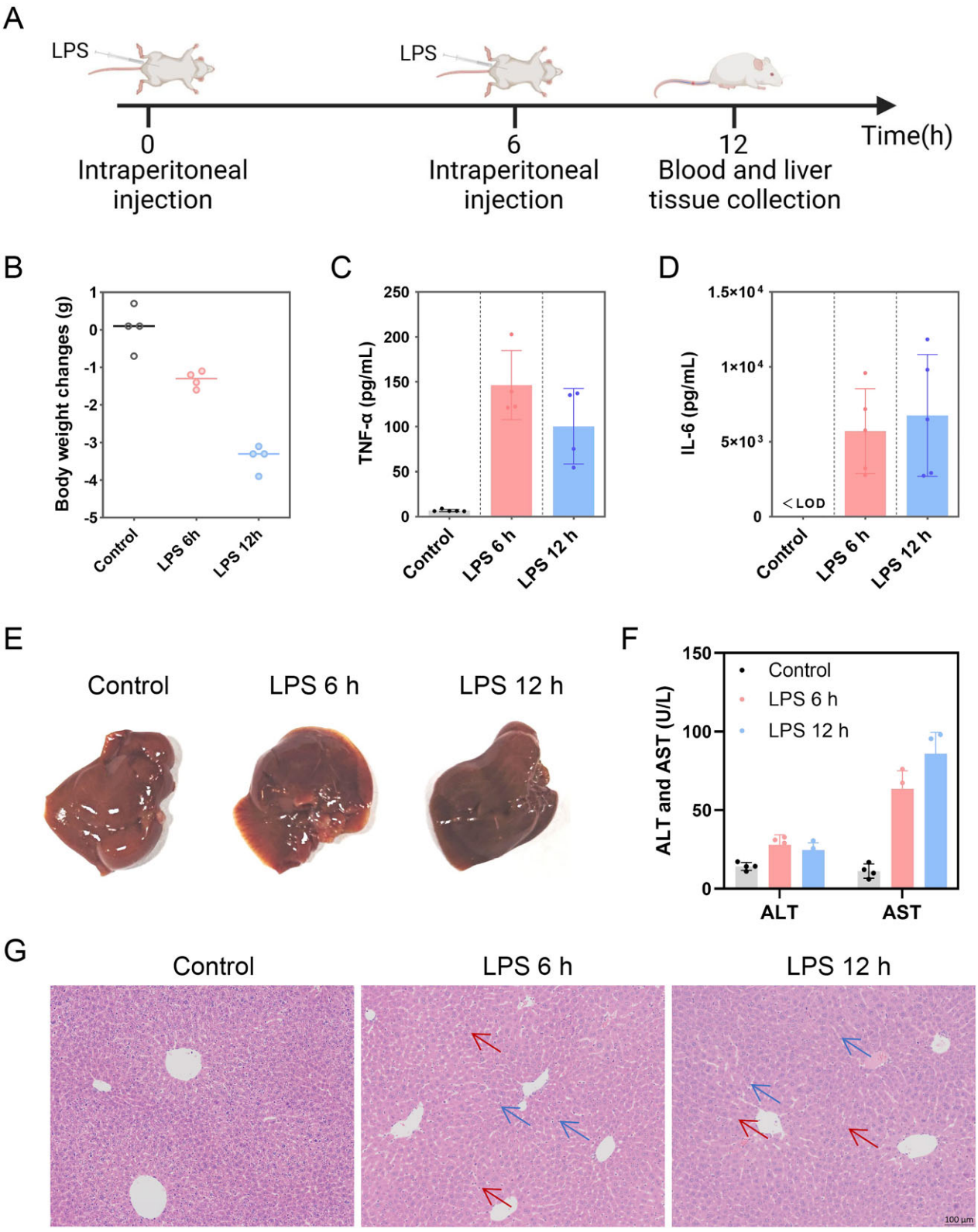

Figure 6. Establishment of an LPS-induced sepsis model in mice. (**A**) Schematic diagram of the LPS-induced sepsis in mice. (**B**) Body weight changes 6 and 12 h after LPS injection in sepsis mouse model ($n = 4$, respectively). Detection of pro-inflammatory factors TNF-α (**C**) and IL-6 (**D**) in serum of mice under indicated conditions. The "< LOD" indicates values that are less than the limit of detection (LOD). (**E**) Liver color changes in 6 and 12 h after LPS injection in sepsis mouse model. (**F**) The level of ALT and AST changes 6 and 12 h after LPS injection in sepsis mouse model. (**G**) HE staining of mice livers in sepsis mouse model. The red arrows indicate obscure nuclei of hepatocytes. The blue arrows indicate hepatocytes with vacuolar degeneration.

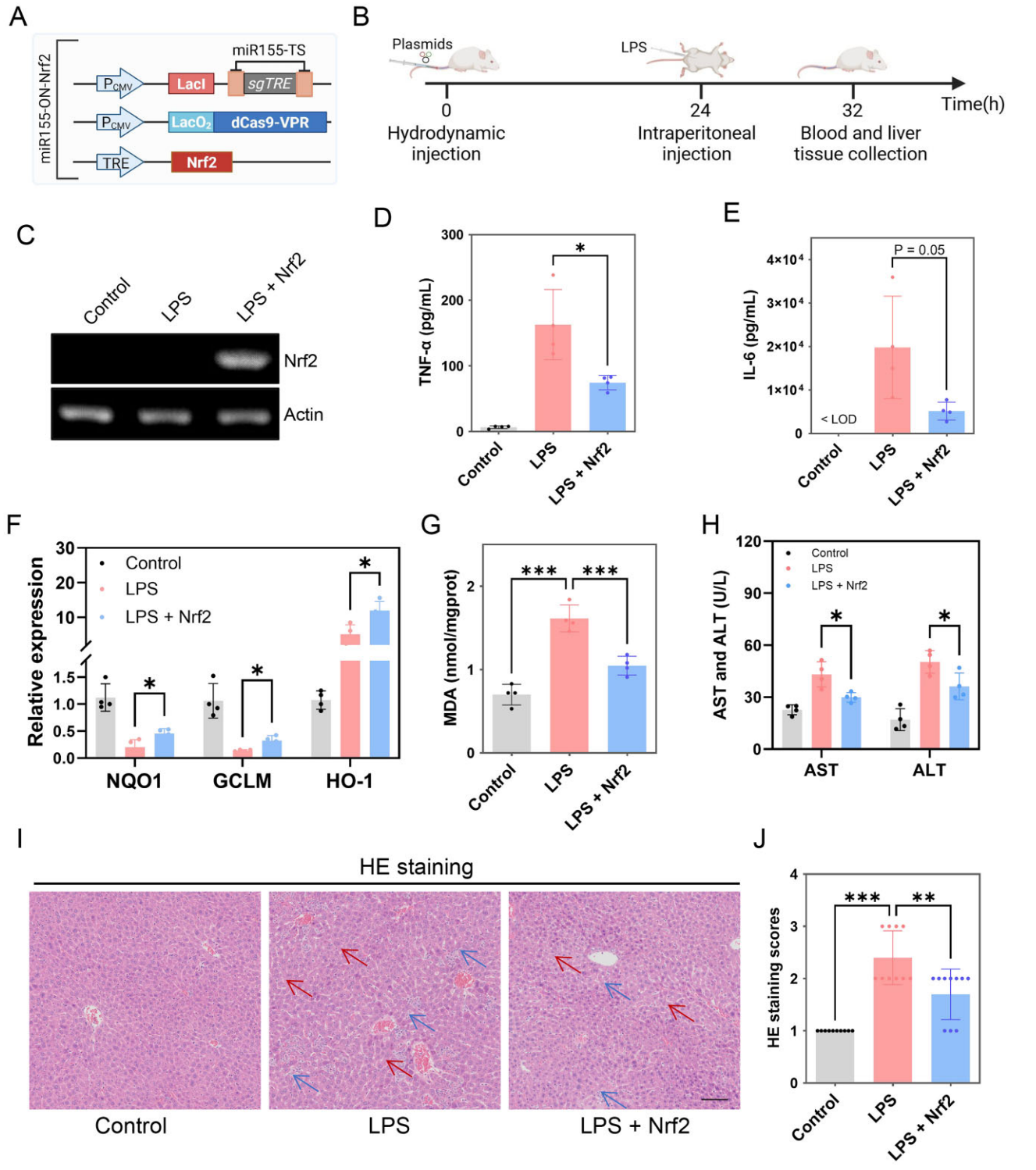

Figure 7. miR-ON-CRISPR system activates the expression of Nrf2 to alleviate sepsis-induced liver injury in mice. (**A**) Schematic diagram of the components of the miR155-ON-Nrf2 system. (**B**) Experimental diagram to explore the role of the miR155-ON-Nrf2 system in LPS-induced sepsis. (**C**) The expression of Nrf2 was detected by RT-PCR. The label "LPS + Nrf2" in the figure indicates the expression of the miR155-ON-Nrf2 system plasmids in LPS-induced sepsis mice (same below). Detection of pro-inflammatory factors TNF-α (**D**) and IL-6 (**E**) in serum of mice under different conditions. The "< LOD" indicates values that are less than the LOD. (**F**) The expression of several antioxidized genes was detected by RT-qPCR. (**G**) Detection of MDA levels in mouse liver tissue. (**H**) Detection of AST and ALT in serum of mice under different conditions. (**I** and **J**) Representative HE staining images of mice livers and staining scores. The red arrows indicate obscure nuclei of hepatocytes. The blue arrows indicate hepatocytes with vacuolar degeneration. Scale bar: 100 μm.

miR155-ON-Nrf2 system may alleviate sepsis-induced liver injury. Indeed, in sepsis mice expressing the miR155-ON-Nrf2 system plasmids, the biomarkers ALT and AST in serum for reflecting liver injury were both decreased (Fig. 7H). In line with this observation, the HE staining scores were significantly higher in the liver tissues of LPS-induced sepsis mice compared with the control group, whereas the expression of the miR155-ON-Nrf2 system could suppress the increased staining scores (Fig. 7I and J). Taken together, these data demonstrated that the miR-ON-CRISPR system has the capacity to alleviate sepsis-induced liver injury in mice.

Conclusion

In this study, we have developed an miRNA-inducible CRISPR–dCas9 dual regulatory system in which both dCas9 and sgRNA production are regulated by endogenous miRNA signature. The configuration of this dual regulatory mechanism ensures that the CRISPR system activity is tightly regulated by cell type-specific target miRNAs, thereby reducing off-target effects and genotoxicity by minimizing the exposure time of the genome to the active system. The efficacy of the robust system in measuring miRNA activity and monitoring the neural cell differentiation was demonstrated. Furthermore, by designing sgRNAs that target the promoter region of exogenous or endogenous apoptosis-related genes, we successfully adapted this system to achieve cell type-specific killing. Finally, it was shown that liver injury in sepsis can be alleviated by employing the system to induce the expression of Nrf2 in the liver of mice, thereby substantiating the system's efficacy *in vivo*. These results highlight the utility of this CRISPR–dCas9 dual regulatory system for the detection of miRNA and the specific activation of genes, either in terms of cell type or disease state, suggesting its potential application in both fundamental biological research and gene-based therapeutic interventions.

While we do demonstrate miR-ON-CRISPR system application for gene-based therapy by using the LPS-induced model, the present paper merely reports the initial proof-of-principle study. Given that miR-ON-CRISPR is a fully genetically encoded system, a variety of vectors and tissue-specific promoters could be used to selectively deliver miR-ON-CRISPR system components to diverse tissues. Besides, we also envision that adeno-associated virus vectors will become the prevailing approach for this task. Moreover, the miR-ON-CRISPR system is modular and programmable, and thus is also applicable to other CRISPR systems, such as the CRISPR–Cas12a system. Furthermore, it is important to note that the occurrence of some diseases often involves multiple different changes in miRNA expression. However, the current system can only respond to one or two miRNAs, which may limit its application in gene therapy scenarios. To achieve precise gene-based therapy, developing a CRISPR system that can respond to the expression of multiple miRNAs is of great significance.

Acknowledgements

Schematic figures were created in BioRender. Ma, E. (2025) https://BioRender.com/sjwz59f.

Author contributions: Wen-Jie Shu (Formal analysis [lead], Methodology [lead], Software [equal], Visualization [lead], Writing—original draft [equal], Zhe Ma (Formal analysis [equal], Investigation [equal], Methodology [equal], Validation [equal]), Lijun Jia (Investigation [equal], Methodology [equal], Resources [equal]), Bin Guo (Investigation [equal], Methodology [equal], Resources [equal]), Xiaojie Tian (Investigation [equal], Methodology [equal]), Chunxia He (Investigation [equal], Methodology [equal]), and Fu Wang (Conceptualization [Lead], Writing—review & editing [Lead], Funding acquisition [Lead], Project administration [Lead], Supervision [Lead]).

Supplementary data

Supplementary data is available at NAR online.

Conflict of interest

None declared.

Funding

This work was supported by grants from the National Natural Science Foundation of China (Nos. 32271512, 82572281, and 32201199), Natural Science Basic Research Program of Shaanxi (Nos. 2023-JC-ZD-43, 2025JC-YBQN-1129, 2022JC-56), the Key Research and Development Program of Shaanxi (No. 2024SF-YBXM-138), the Young Talent Fund of Xi'an Association for Science and Technology (No. 0959202513035), and Xi'an Science and Technology Research Program (No. 24YXYJ0031). Funding to pay the Open Access publication charges for this article was provided by National Natural Science Foundation of China.

Data availability

All relevant data are included in the paper and/or its supplementary information files.

References

1. Fal K, Carles CC. dCas-based tools to visualize chromatin or modify epigenetic marks at specific plant genomic loci. *Methods Mol Biol* 2025;**2873**:305–32. https://doi.org/10.1007/978-1-0716-4228-3_17
2. Rajanathadurai J, Perumal E, Sindya J. Advances in targeting cancer epigenetics using CRISPR–dCas9 technology: a comprehensive review and future prospects. *Funct Integr Genomics* 2024;**24**:164. https://doi.org/10.1007/s10142-024-01455-3
3. Mahas A, Neal Stewart C Jr, Mahfouz MM. Harnessing CRISPR/Cas systems for programmable transcriptional and post-transcriptional regulation. *Biotechnol Adv* 2018;**36**:295–310. https://doi.org/10.1016/j.biotechadv.2017.11.008
4. Zhang H, Zhu JK. Epigenetic gene regulation in plants and its potential applications in crop improvement. *Nat Rev Mol Cell Biol* 2025;**26**:51–67. https://doi.org/10.1038/s41580-024-00769-1
5. Zhou W, Deiters A. Conditional control of CRISPR/Cas9 function. *Angew Chem Int Ed Engl* 2016;**55**:5394–9. https://doi.org/10.1002/anie.201511441
6. Cai W, Wang M. Engineering nucleic acid chemistry for precise and controllable CRISPR/Cas9 genome editing. *Sci Bull* 2019;**64**:1841–9. https://doi.org/10.1016/j.scib.2019.07.035
7. Wang X, Dong K, Kong D *et al.* A far-red light-inducible CRISPR–Cas12a platform for remote-controlled genome editing and gene activation. *Sci Adv* 2021;**7**:eabh2358. https://doi.org/10.1126/sciadv.abh2358

8. Yu Y, Wu X, Guan N *et al.* Engineering a far-red light-activated split-Cas9 system for remote-controlled genome editing of internal organs and tumors. *Sci Adv* 2020;**6**:eabb1777. https://doi.org/10.1126/sciadv.abb1777
9. Chen S, Chen D, Liu B *et al.* Modulating CRISPR/Cas9 genome-editing activity by small molecules. *Drug Discov Today* 2022;**27**:951–66. https://doi.org/10.1016/j.drudis.2021.11.018
10. Shang R, Lee S, Senavirathne G *et al.* microRNAs in action: biogenesis, function and regulation. *Nat Rev Genet* 2023;**24**:816–33. https://doi.org/10.1038/s41576-023-00611-y
11. He B, Zhao Z, Cai Q *et al.* miRNA-based biomarkers, therapies, and resistance in cancer. *Int J Biol Sci* 2020;**16**:2628–47. https://doi.org/10.7150/ijbs.47203
12. Shu WJ, Lee K, Ma Z *et al.* A dual-regulation inducible switch system for microRNA detection and cell type-specific gene activation. *Theranostics* 2023;**13**:2552–61. https://doi.org/10.7150/thno.84111
13. Zhang C, Shi X, Tang C *et al.* Engineering synthetic CopT/A-based genetic biosensors for miRNA imaging and functional gene regulation. *Anal Chem* 2023;**95**:6748–56. https://doi.org/10.1021/acs.analchem.3c00873
14. Zhang C, Zhang B, Tang C *et al.* A ratiometric gene-switch system for miRNA sensing and gene regulation. *Small Methods* 2024;**8**:e2301266. https://doi.org/10.1002/smtd.202301266
15. Hu C, Shi X, Guo B *et al.* Toehold-based CRISPR–dCas9 transcriptional activation platform for spatiotemporally controllable gene therapy in tumor and diabetic mouse models. *ACS Nano* 2025;**19**:12277–87. https://doi.org/10.1021/acsnano.5c01078
16. Hoffmann MD, Aschenbrenner S, Grosse S *et al.* Cell-specific CRISPR–Cas9 activation by microRNA-dependent expression of anti-CRISPR proteins. *Nucleic Acids Res* 2019;**47**:e75. https://doi.org/10.1093/nar/gkz271
17. Hirosawa M, Fujita Y, Parr CJC *et al.* Cell-type-specific genome editing with a microRNA-responsive CRISPR–Cas9 switch. *Nucleic Acids Res* 2017;**45**:e118. https://doi.org/10.1093/nar/gkx309
18. Oesinghaus L, Simmel FC. Controlling gene expression in mammalian cells using multiplexed conditional guide RNAs for Cas12a*. *Angew Chem Int Ed Engl* 2021;**60**:23894–902. https://doi.org/10.1002/anie.202107258
19. Wang XW, Hu LF, Hao J *et al.* A microRNA-inducible CRISPR–Cas9 platform serves as a microRNA sensor and cell-type-specific genome regulation tool. *Nat Cell Biol* 2019;**21**:522–30. https://doi.org/10.1038/s41556-019-0292-7
20. Wang W-J, Lin J, Wu C-Q *et al.* Establishing artificial gene connections through RNA displacement–assembly-controlled CRISPR/Cas9 function. *Nucleic Acids Res* 2023;**51**:7691–703. https://doi.org/10.1093/nar/gkad558
21. Shu WJ, Ma Z, Tian XJ *et al.* Near-infrared fluorescence imaging of miRNA using a transmembrane polypeptide-based genetic reporter. *Small Methods* 2024;**8**:e2300990. https://doi.org/10.1002/smtd.202300990
22. Ning H, Liu G, Li L *et al.* Rational design of microRNA-responsive switch for programmable translational control in mammalian cells. *Nat Commun* 2023;**14**:7193. https://doi.org/10.1038/s41467-023-43065-w
23. Miki K, Endo K, Takahashi S *et al.* Efficient detection and purification of cell populations using synthetic microRNA switches. *Cell Stem Cell* 2015;**16**:699–711. https://doi.org/10.1016/j.stem.2015.04.005
24. Hirosawa M, Fujita Y, Saito H. Cell-type-specific CRISPR activation with microRNA-responsive AcrllA4 switch. *ACS Synth Biol* 2019;**8**:1575–82. https://doi.org/10.1021/acssynbio.9b00073
25. Ma D, Peng S, Xie Z. Integration and exchange of split dCas9 domains for transcriptional controls in mammalian cells. *Nat Commun* 2016;**7**:13056. https://doi.org/10.1038/ncomms13056
26. Hunt VM, Chen W. A microRNA-gated thgRNA platform for multiplexed activation of gene expression in mammalian cells. *Chem Commun* 2022;**58**:6215–8. https://doi.org/10.1039/d2cc01478e
27. Hsu PD, Scott DA, Weinstein JA *et al.* DNA targeting specificity of RNA-guided Cas9 nucleases. *Nat Biotechnol* 2013;**31**:827–32. https://doi.org/10.1038/nbt.2647
28. Doench JG, Fusi N, Sullender M *et al.* Optimized sgRNA design to maximize activity and minimize off-target effects of CRISPR-Cas9. *Nat Biotechnol* 2016;**34**:184–91. https://doi.org/10.1038/nbt.3437
29. Chavez A, Scheiman J, Vora S *et al.* Highly efficient Cas9-mediated transcriptional programming. *Nat Methods* 2015;**12**:326–8. https://doi.org/10.1038/nmeth.3312
30. Sano M, Morishita K, Oikawa S *et al.* Live-cell imaging of microRNA expression with post-transcriptional feedback control. *Mol Ther Nucleic Acids* 2021;**26**:547–56. https://doi.org/10.1016/j.omtn.2021.08.018
31. Kulsoom AW, Wang F. Advancement in synthetic gene circuits engineering: an alternative strategy for microRNA imaging and disease theranostics. *Biotechnol Adv* 2025;**79**:108518. https://doi.org/10.1016/j.biotechadv.2025.108518
32. Matsuura S, Ono H, Kawasaki S *et al.* Synthetic RNA-based logic computation in mammalian cells. *Nat Commun* 2018;**9**:4847. https://doi.org/10.1038/s41467-018-07181-2
33. Kato Y. Extremely low leakage expression systems using dual transcriptional-translational control for toxic protein production. *Int J Mol Sci* 2020;**21**:705. https://doi.org/10.3390/ijms21030705
34. Strnad P, Tacke F, Koch A *et al.* Liver—guardian, modifier and target of sepsis. *Nat Rev Gastroenterol Hepatol* 2017;**14**:55–66. https://doi.org/10.1038/nrgastro.2016.168
35. Nesseler N, Launey Y, Aninat C *et al.* Clinical review: the liver in sepsis. *Crit Care* 2012;**16**:235. https://doi.org/10.1186/cc11381
36. Li L, Zhang Q, Zhang X *et al.* Protective effects of Nrf2 against sepsis-induced hepatic injury. *Life Sci* 2021;**282**:119807. https://doi.org/https://doi.org/10.1016/j.lfs.2021.119807
37. Dai JM, Guo WN, Tan YZ *et al.* Wogonin alleviates liver injury in sepsis through Nrf2-mediated NF-κB signalling suppression. *J Cell Mol Med* 2021;**25**:5782–98. https://doi.org/10.1111/jcmm.16604
38. Bindayna K. MicroRNA as sepsis biomarkers: a comprehensive review. *Int J Mol Sci* 2024;**25**:6476. https://doi.org/10.3390/ijms25126476
39. Yang ZB, Chen WW, Chen HP *et al.* MiR-155 aggravated septic liver injury by oxidative stress-mediated ER stress and mitochondrial dysfunction via targeting Nrf-2. *Exp Mol Pathol* 2018;**105**:387–94. https://doi.org/10.1016/j.yexmp.2018.09.003
40. Chen M, Wang F, Xia H *et al.* MicroRNA-155: regulation of immune cells in sepsis. *Mediators Inflamm* 2021;**2021**:8874854. https://doi.org/10.1155/2021/8874854
41. Jaeschke H. Reactive oxygen and mechanisms of inflammatory liver injury: present concepts. *J Gastroenterol Hepatol* 2011;**26**:173–9. https://doi.org/10.1111/j.1440-1746.2010.06592.x
42. Khan NM, Haseeb A, Ansari MY *et al.* Wogonin, a plant derived small molecule, exerts potent anti-inflammatory and chondroprotective effects through the activation of ROS/ERK/Nrf2 signaling pathways in human Osteoarthritis chondrocytes. *Free Radic Biol Med* 2017;**106**:288–301. https://doi.org/10.1016/j.freeradbiomed.2017.02.041
43. Tang Q, Zheng G, Feng Z *et al.* Trehalose ameliorates oxidative stress-mediated mitochondrial dysfunction and ER stress via selective autophagy stimulation and autophagic flux restoration in osteoarthritis development. *Cell Death Dis* 2017;**8**:e3081. https://doi.org/10.1038/cddis.2017.453

Received: June 25, 2025. **Revised:** September 18, 2025. **Accepted:** September 19, 2025